Supporting Information for

Elemental fingerprint as a potential tool for tracking the fate of real-life model nanoplastics generated from plastic consumer products in environmental systems

Mohammed Baalousha[1]*, Jingjing Wang[1], Md Mahmudun Nabi[1], Mahbub Alam[1], Mahdi Erfani[2], Julien Gigault[3], Florent Blancho[4], Mélanie Davranche[4], Phillip Potter[5], Souhail R. Al-Abed[5]

Affiliations:

[1] Center for Environmental Nanoscience and Risk, Department of Environmental Health Sciences, Arnold School of Public Health, University of South Carolina, SC 29208, United States

[2] TAKUVIK Laboratory, CNRS/Université Laval, 1045, av. de La Médecine, Québec G1V 0A6, Canada

[3] Géosciences Rennes, CNRS/Université de Rennes, 263 av. Général Leclerc, 35000 Rennes, France

[4] Office of Research and Development, Center for Environmental Solutions and Emergency Response, US Environmental Protection Agency, 26 W. Martin Luther King Drive, Cincinnati, OH 45268, United States

* Corresponding author: mbaalous@mailbox.sc.edu

1. Elemental analysis by SP-ICP-TOF-MS

Table S1. Operating conditions for inductively coupled plasma-time of flight-mass spectrometer analysis (TOFWERK icpTOF R) for conventional (dissolved metal concentration) and single particle analysis modes.

<table>
<tr><th>Instrument parameter</th><th colspan="5">Total concentration analysis</th><th colspan="5">Single particle analysis</th></tr>
<tr><td>Plasma Power</td><td colspan="5">1550 W</td><td colspan="5">1550 W</td></tr>
<tr><td>Nebulizer Gas Flow</td><td colspan="5">1.10-1.14 L/min</td><td colspan="5">1.10-1.14 L/min</td></tr>
<tr><td>Auxiliary Gas Flow</td><td colspan="5">0.8 L/min</td><td colspan="5">0.8 L/min</td></tr>
<tr><td>Cooling Gas Flow</td><td colspan="5">14 L/min</td><td colspan="5">14 L/min</td></tr>
<tr><td>Injector Diameter</td><td colspan="5">2.5 mm</td><td colspan="5">2.5 mm</td></tr>
<tr><td>Collision Cell Gas</td><td colspan="5">5 mL/min He with 4.5% H_2</td><td colspan="5">5 mL/min He with 4.5% H_2</td></tr>
<tr><td>CCT Bias</td><td colspan="5">-2.00 to -4.00 V</td><td colspan="5">-2.00 to -4.00 V</td></tr>
<tr><td rowspan="2">Notch</td><td>Mass</td><td>29</td><td>32</td><td>36.3</td><td>41</td><td>Mass</td><td>29</td><td>32</td><td>36.3</td><td>41</td></tr>
<tr><td>Amplitude (V)</td><td>1.6</td><td>2.0</td><td>2.0</td><td>1.2</td><td>Amplitude (V)</td><td>1.6</td><td>2.0</td><td>2.0</td><td>1.2</td></tr>
<tr><td>TOF Repetition Rate</td><td colspan="5">33 kHz</td><td colspan="5">33 kHz</td></tr>
<tr><td>Detected Mass Range</td><td colspan="5">14-275 m/Z</td><td colspan="5">14-275 m/Z</td></tr>
<tr><td>(CeO/Ce)</td><td colspan="5">< 4.0%</td><td colspan="5">< 4.0%</td></tr>
<tr><td>Data Acquisition</td><td colspan="5">Continuous Mode</td><td colspan="5">Continuous Mode</td></tr>
<tr><td>TOF Time Resolution</td><td colspan="5">0.3 s</td><td colspan="5">30 µs</td></tr>
<tr><td>Integration Time</td><td colspan="5">0.3 s</td><td colspan="5">2 ms</td></tr>
<tr><td>Acquisition Time</td><td colspan="5">60 s</td><td colspan="5">200-300 s</td></tr>
<tr><td>Sample Flow Rate</td><td colspan="5">-</td><td colspan="5">0.455 mL/min</td></tr>
<tr><td>Transport Efficiency</td><td colspan="5">-</td><td colspan="5">6.6% (5-7%)</td></tr>
</table>

Table S2. Elements monitored for single particle-inductively coupled plasma-time of flight-mass spectrometer analysis and the corresponding particle mass and size detection limits.

Element	Isotope	Mass detection limit (g)	Size detection limit (nm)	Size detection limit (nm)	Metal oxide formulae
Al	^{27}Al	8.30×10^{-15}	180	196	Al_2O_3
Si	^{28}Si	2.95×10^{-14}	289	357	SiO_2
Ti	^{48}Ti	5.57×10^{-16}	62	75	TiO_2
V	^{51}V	3.77×10^{-16}	49	73	V_2O_5
Cr	^{52}Cr	3.35×10^{-16}	45	56	Cr_2O_3
Mn	^{55}Mn	2.58×10^{-16}	41	54	MnO_2
Fe	^{56}Fe	3.27×10^{-16}	43	55	Fe_2O_3
Co	^{59}Co	2.08×10^{-16}	35	45	Co_3O_4
Ni	^{60}Ni	8.55×10^{-16}	57	68	NiO
Cu	^{65}Cu	6.80×10^{-16}	53	64	CuO
Zn	^{66}Zn	1.53×10^{-15}	74	87	ZnO
Zr	^{90}Zr	1.57×10^{-16}	36	41	ZrO_2
Nb	^{93}Nb	8.25×10^{-17}	26	36	Nb_2O_5
Sn	^{120}Sn	1.43×10^{-16}	33	37	SnO_2
Sb	^{121}Sb	1.83×10^{-16}	37	43	Sb_2O_3
Ba	^{138}Ba	6.85×10^{-17}	33	29	BaO
La	^{139}La	4.55×10^{-17}	24	25	La_2O_3
Ce	^{140}Ce	4.89×10^{-17}	24	25	CeO_2
Pr	^{141}Pr	3.81×10^{-17}	22	24	Pr_6O_{11}
Nd	^{144}Nd	1.01×10^{-16}	30	31	Nd_2O_3
Sm	^{152}Sm	1.17×10^{-16}	31	31	Sm_2O_3
Eu	^{153}Eu	5.98×10^{-17}	28	26	Eu_2O_3
Gd	^{158}Gd	1.32×10^{-16}	32	34	Gd_2O_3
Tb	^{159}Tb	3.20×10^{-17}	20	21	Tb_4O_7
Dy	^{164}Dy	9.74×10^{-17}	28	30	Dy_2O_3
Ho	^{165}Ho	2.92×10^{-17}	18	20	Ho_2O_3
Er	^{166}Er	8.80×10^{-17}	26	28	Er_2O_3
Tm	^{169}Tm	2.95×10^{-17}	18	20	Tm_2O_3
Yb	^{174}Yb	8.27×10^{-17}	29	27	Yb_2O_3
Lu	^{175}Lu	2.67×10^{-17}	17	18	Lu_2O_3
Hf	^{180}Hf	6.34×10^{-17}	21	25	HfO_2
Ta	^{181}Ta	2.66×10^{-17}	14	20	Ta_2O_5
W	^{184}W	9.11×10^{-17}	21	27	WO_2
Pb	^{208}Pb	6.23×10^{-17}	22	24	PbO
Th	^{232}Th	2.93×10^{-17}	17	19	ThO_2
U	^{238}U	2.85×10^{-17}	14	18	UO_2

Particle mass detection limit is calculated according to the Poisson distribution =
$Mass_{detection\ limit} = 3.29\sqrt{background\ signal} + 2.71$

Size detection limit is calculated as the equivalent spherical diameter from the particle mass detection limit assuming pure metal and metal oxide phases

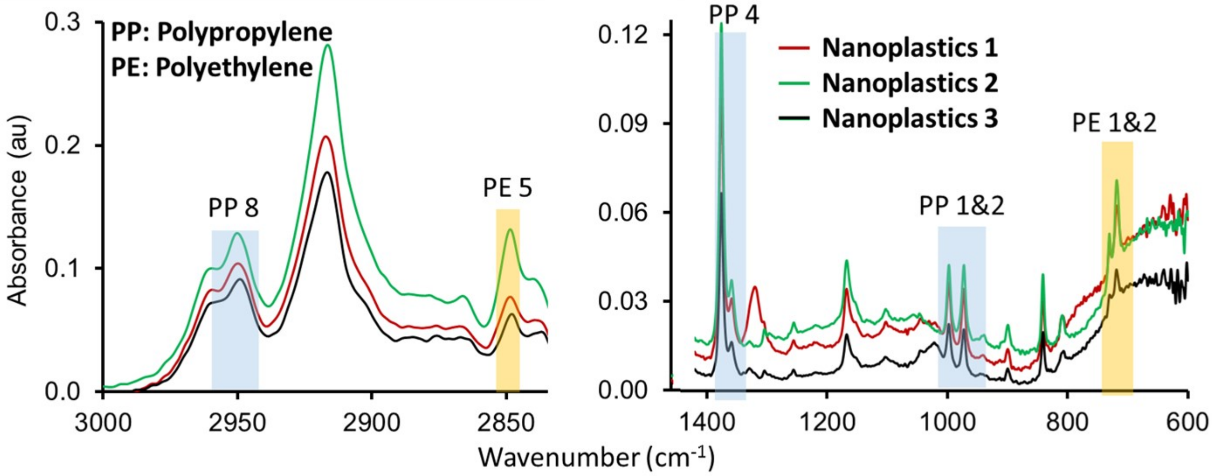

2.
3. **Figure S1.** Fourier transform-infrared (FT-IR) spectra of the model real life nanoplastics generated from ocean aged plastic fragments (NPO) collected from the North Atlantic garbage patch. For polyethylene, the specific bands PE 1&2 at 675 cm^{-1} and PE 5 at 2850 cm^{-1} correspond to the specific perpendicular deformation of the CH2 and the symmetrical vibration of the C-H, respectively; PP1&2 at 996 and 1166cm^{-1} correspond to the rocking CH3 while the PP 4 at 1376 cm^{-1} is the symmetrical bending of the CH3 and the PP8 is the asymmetrical stretching of the CH3.

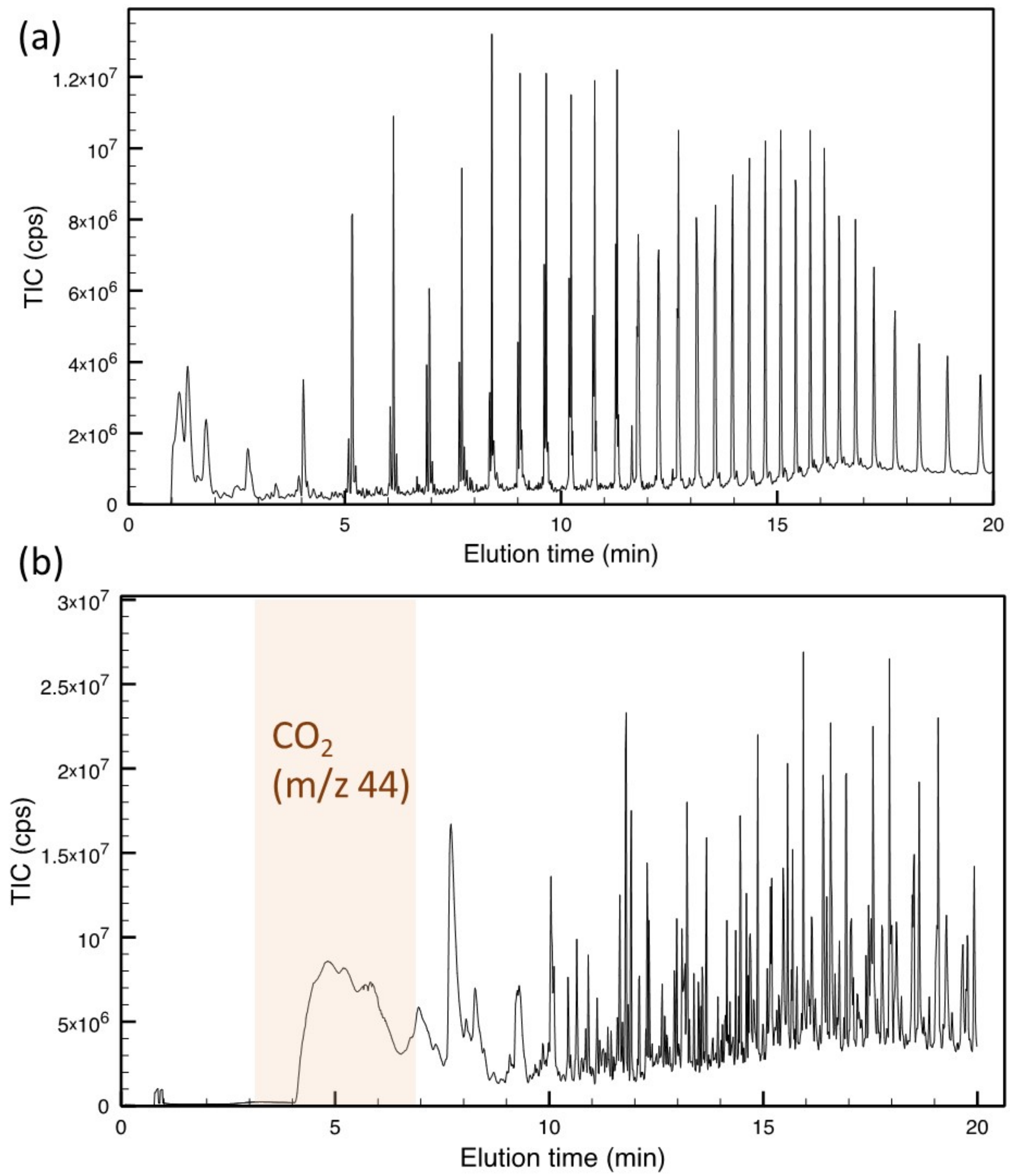

Figure S2. Total Ion Counts (TIC) pyrograms for (a) Nanoplastics 1 and (b) Nanoplastics 4, performed at 600 °C in the optimized conditions described in the material and methods section. For Nanoplastics 1, the alkene compounds are clearly identified without extracting the m/z as described in the main text. For Nanoplastics 4, the TIC pyrogram illustrates a large composition heterogeneity, including natural organic matter, propylene, and trace of polyethylene. It is worth noting that a large signal appears on the Nanoplastics 4 pyrogram and corresponds to the carbon dioxide. The formation of carbon dioxide is a strong indicator of the presence of natural organic matter in the pyrolysis cup, which confirms the largest heterogeneity in the colloidal composition for Nanoplastics 4. Spectra for Nanoplastics 2, and 3 are not presented as they the same as those for Nanoplastics 1.

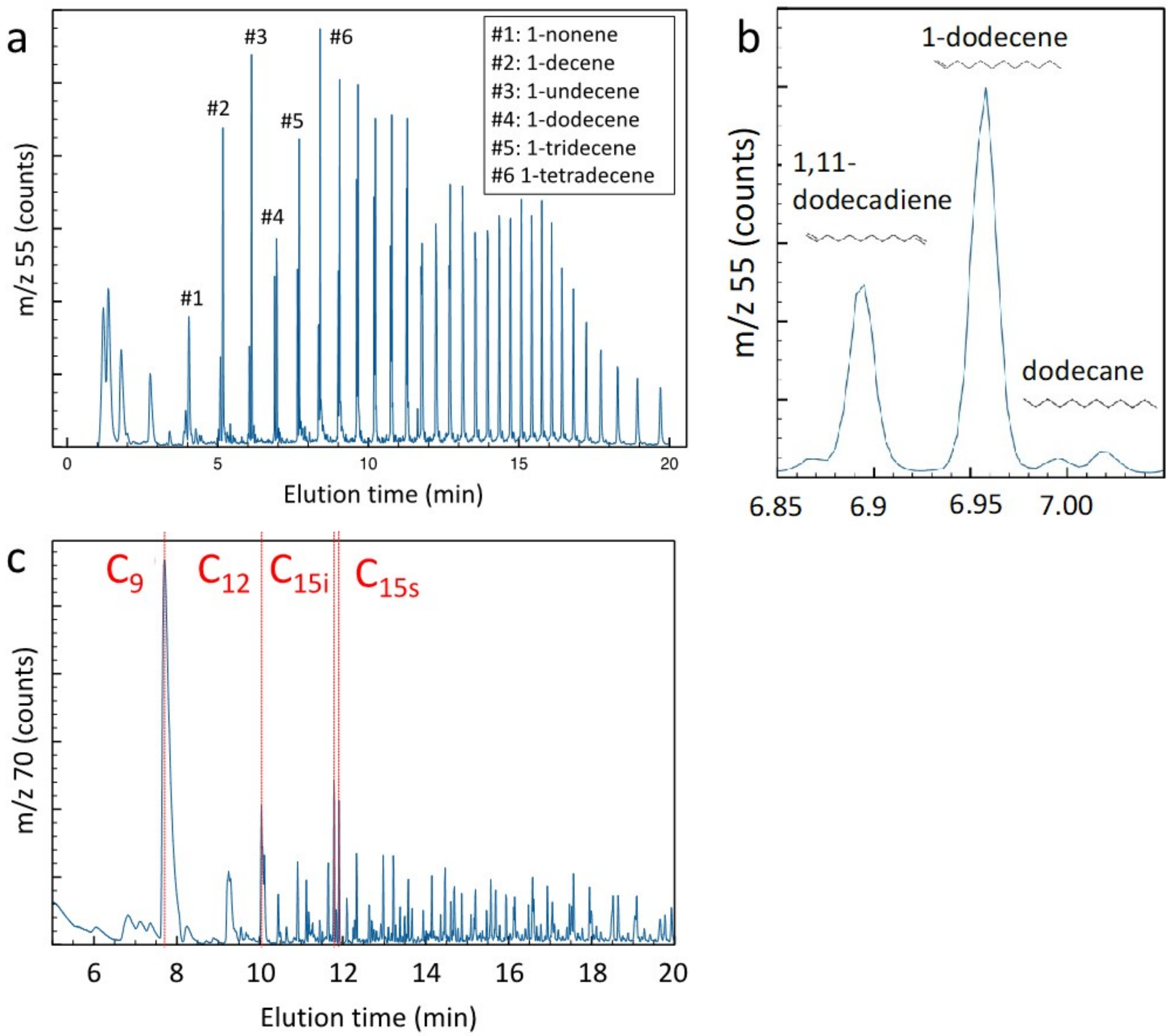

Figure S3. Pyrolysis GC-MS pyrograms of (a) m/z 55 for the Nanoplastics 1 obtained using a 30m DB5-MS C18 column, (b) zoom in on the dodecadiene/dodecane/dodecane peaks, and (c) m/z 70 of the Nanoplastics 4 with the markers of polypropylene (C9, C12, C15i, and C15s) obtained using a 60m DB5-MS C18 column. Similar results were obtained for Nanoplastics 1, 2 and 3 and are thus spectra for Nanoplastics 2 and Nanoplastics 3 are not presented here. The pyrogram illustrates the elution of pyrolysates (*i.e.,* fragments of macromolecules) formed during the pyrolysis at 600°C.

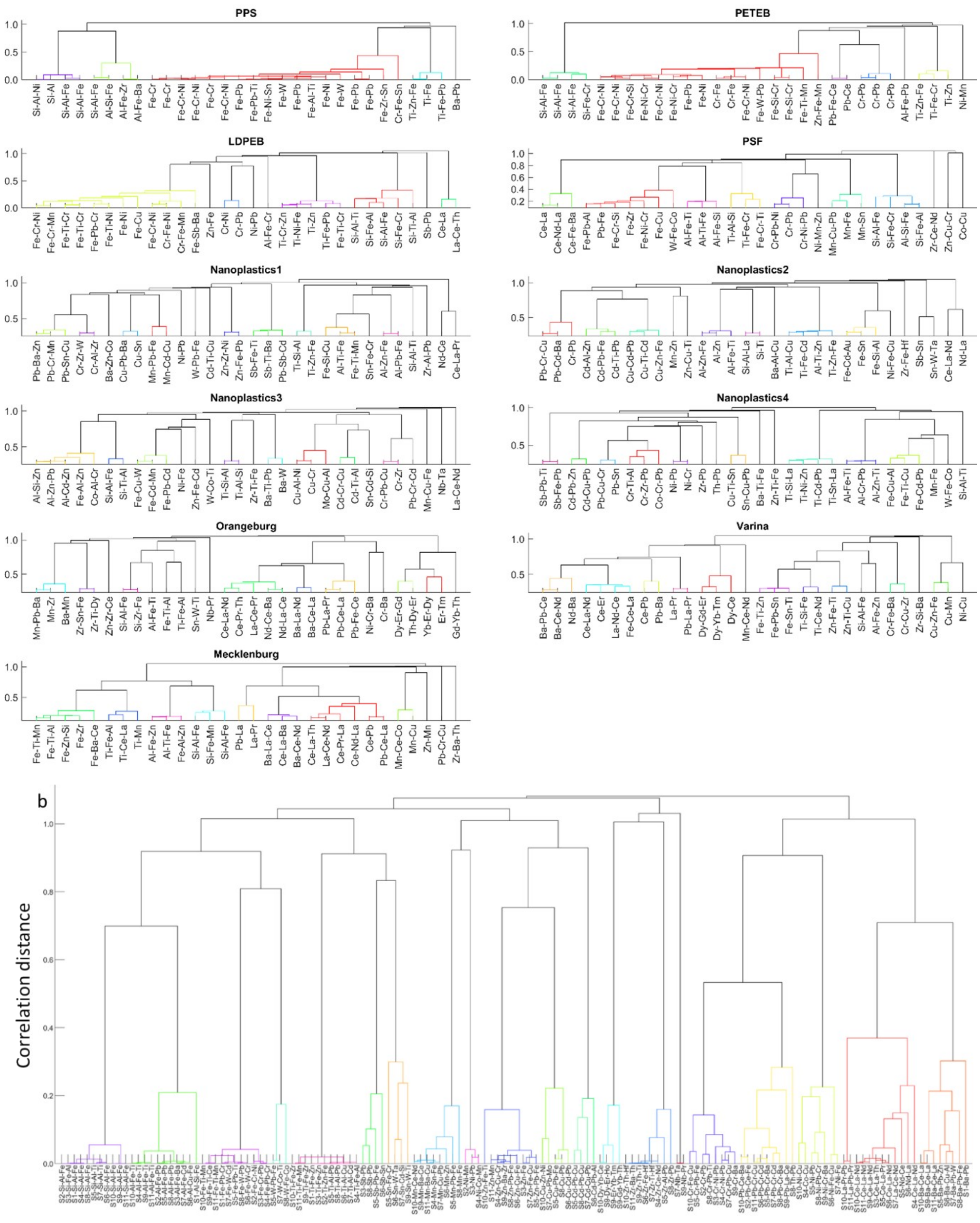

Figure S4. First stage clustering dendrogram. PPS (S1), PETEB (S2), LDBEB (S3), and PSF (S4) refer to the model real-life nanoplastics generated from new plastic products including polypropylene straw, polyethylene terephthalate bottle, white low density polyethylene bag, and polystyrene foam, respectively. Nanoplastics 1 (S5), 2 (S6), 3 (S7), and 4 (S8) refer to the model real-life nanoplastics generated from environmentally aged ocean plastic fragments. Orangeburg (S9), Varina (S10), and Mecklenburg (S11) refer to the three soil samples.

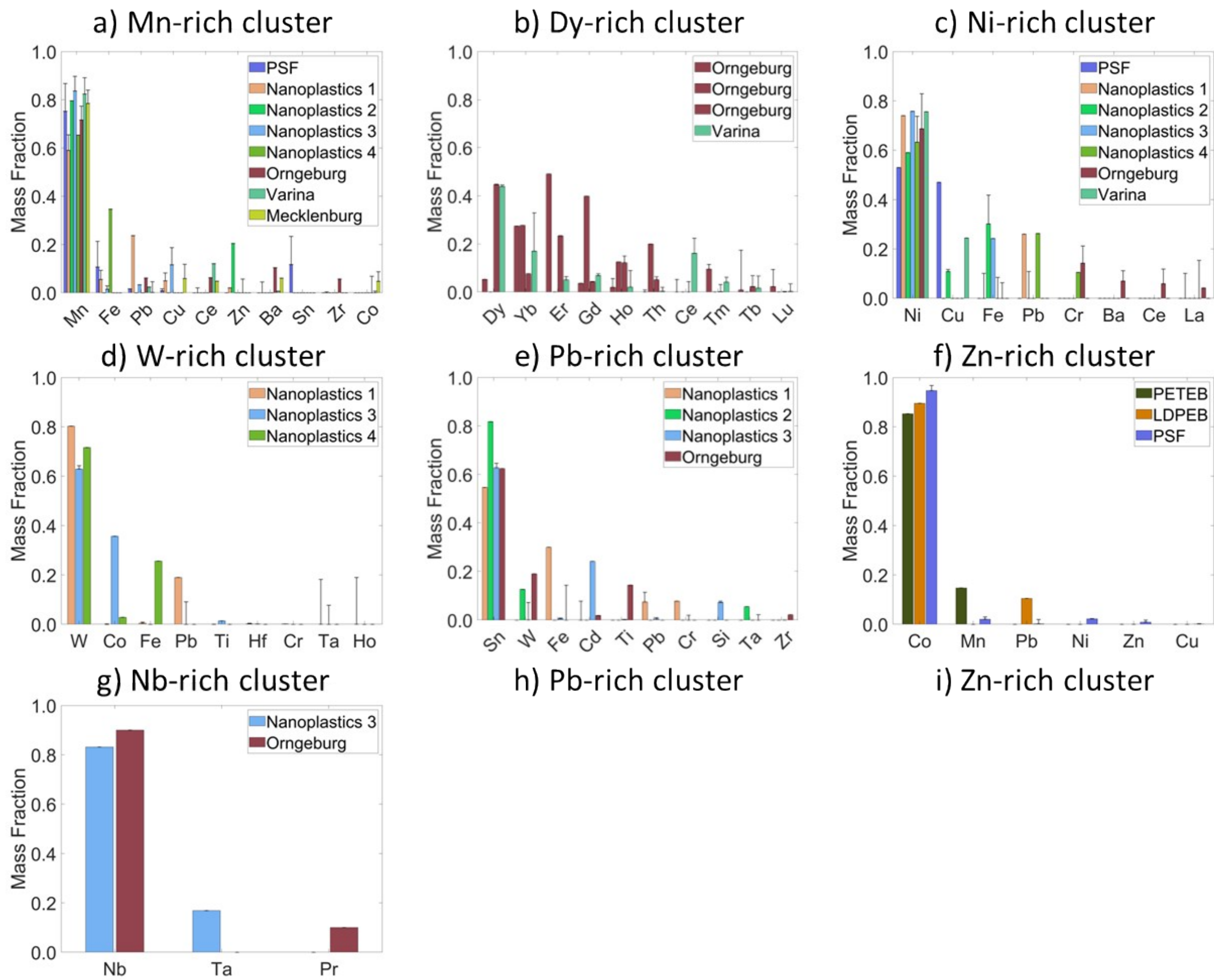

Figure S5. Mean mass fraction of frequent elements within each cluster. PPS, PETEB, LDBEB, and PSF refer to the model real-life nanoplastics generated from new plastic products including polypropylene straw, polyethylene terephthalate bottle, white low density polyethylene bag, and polystyrene foam, respectively. Nanoplastics 1, 2, 3, and 4 refer to the model real-life nanoplastics generated from environmentally aged ocean plastic fragments. Orangeburg, Varina, and Mecklenburg refer to the three soil samples.